

1 **Investigation of deuteron-induced reactions on  $^{\text{nat}}\text{Gd}$  up**  
2 **to 30 MeV: possibility of production of medically**  
3 **relevant  $^{155}\text{Tb}$  and  $^{161}\text{Tb}$  radioisotopes**

4 Ferenc Szelecsényi<sup>1</sup>, Zoltán Kovács<sup>1</sup>, Kotaro Nagatsu<sup>2</sup>, Ming-Rong Zhang<sup>2</sup>, Kazutosi  
5 Suzuki<sup>2</sup>

6 <sup>1</sup>*Cyclotron Application Department, Institute for Nuclear Research of the Hungarian*  
7 *Academy of Sciences, ATOMKI, 18/c Bem tér, H-4026 Debrecen, Hungary*

8 <sup>2</sup>*Molecular Imaging Center, National Institute of Radiological Sciences, NIRS, 4-9-1*  
9 *Anagawa, Inage-ku, Chiba, Japan*

10 **Abstract**

11 Excitation function for the  $^{\text{nat}}\text{Gd}(d,xn)^{155}\text{Tb}$  and  $^{\text{nat}}\text{Gd}(d,n)^{161}\text{Tb}$  nuclear reactions were  
12 measured using the standard stacked-foil activation technique in the deuteron energy  
13 range of 30 MeV down to 4.2 MeV. The measured cross-section data were compared not  
14 only with the earlier reported experimental values but also with the results of a theoretical  
15 model as well. Integral yields for  $^{155}\text{Tb}$  and  $^{161}\text{Tb}$  and for their contaminating  
16 radioisotopes were also deduced to evaluate the production circumstances. The results  
17 revealed that the investigated radioisotopes can not be produced in no-carrier-added form  
18 via deuteron way even using 100% enriched targets ( $^{155}\text{Gd}$  and  $^{160}\text{Gd}$ ).

19

20 **Keywords**

21 Gadolinium target; Terbium radioisotopes; Deuteron irradiation; TENDL 2014 library

## 22 Introduction

23 Recently the element Terbium, member of the lanthanide row, attracted special attention  
24 since it offers a set of radionuclides which are potentially suitable both for therapy and  
25 diagnosis. These radioisotopes possess one or several advantages compared to  
26 radionuclides currently used in radiopharmacy with respect to decay energies and half-  
27 life [1-4]:

28 a) For imaging with PET, the  $^{152g}\text{Tb}$  seems to be a proper candidate. The positron  
29 intensity of 17% (and the mean positron energy of 1.1 MeV) is acceptable. The  
30 only strong gamma line of 344 keV ( $I_{\gamma} = 65\%$ ) is far away from the annihilation  
31 line of 511 keV to avoid coincidence events.

32 c) For targeted particle radionuclide therapy both the  $^{149}\text{Tb}$  ( $T_{1/2} = 4.1$  h,  $I_{\alpha} =$   
33  $17\%$ ) and  $^{161}\text{Tb}$  ( $T_{1/2} = 6.89$  d,  $I_{\beta-} = 100\%$ ) seems to be promising.  $^{161}\text{Tb}$  has a  
34 similar half-life and beta energy as the already useful  $^{177}\text{Lu}$ .

35 c) For diagnostic imaging the  $^{155}\text{Tb}$  seems to be an ideal nuclide. Its half-life (5.32  
36 d) is long enough to observe even slower metabolic processes. The gamma  
37 energies of 87 and 105 keV are ideal for most SPECT cameras.

38 Despite of the opportunity, only a few in vivo applications of Tb-radionuclides are  
39 reported particularly using  $^{152}\text{Tb}$  and  $^{155}\text{Tb}$  [1-3]. The widespread application of Tb-  
40 labeled macromolecules is limited because of the lack of well established and reasonable  
41 production routes of the Terbium radioisotopes. In the case of  $^{155}\text{Tb}$  Levin *et al.* [5] have  
42 already investigated its formation via the  $^{156}\text{Dy}(\gamma,n)^{155}\text{Dy} \rightarrow ^{155}\text{Tb}$  route. Although relative  
43 high radionuclidic purity ( $>99.9\%$ ) was obtained, the available yields are not enough for  
44 practical purposes. For  $^{161}\text{Tb}$ , large-scale production method was developed using highly  
45 enriched  $^{160}\text{Tb}$  as target and intensive neutron beam from a research reactor [1, 6]. Heavy  
46 ions ( $^{12}\text{C}$ -beam) induced nuclear reactions can be also employed for  $^{149}\text{Tb}$  formation  
47 however, the accessibility of this type of beam with high intensity, is very limited [7-9].  
48 Proton-induced spallation of Tantalum target, followed by an online isotope separation  
49 process, seems to be useful for high scale productions of  $^{149,152,155}\text{Tb}$ , however, the

50 number of laboratories equipped with these devices is very limited [1]. Nowadays several  
51 laboratories are involved in research to elaborate practical production methods of the  
52 above Terbium radioisotopes using light charged-particle accelerators [10-13].

53 This study reports on the work of a collaboration established to measure production cross  
54 sections for the formation of medically relevant Terbium radioisotopes using deuterons  
55 available from commercial medical cyclotrons (*e.g.* 30/15 and 18/9 MeV for protons/  
56 deuterons) and enriched Gadolinium targets. Detailed cross-section measurements are  
57 presented here for the  ${}^{\text{nat}}\text{Gd}(d,xn){}^{155,156}\text{Tb}$  and  ${}^{\text{nat}}\text{Gd}(d,xn){}^{160,161}\text{Tb}$  nuclear processes up to  
58 20 MeV. Based on the reliable excitation functions, we calculate also the available yields  
59 for  ${}^{155}\text{Tb}$  and  ${}^{161}\text{Tb}$  to estimate their possible production circumstances. Until now only  
60 Tárkányi *et al.* [10, 11] reported cross sections for  ${}^{\text{nat}}\text{Gd}+d$  processes resulting different  
61 Tb, Gd and Eu radioisotopes including  ${}^{155}\text{Tb}$  and  ${}^{161}\text{Tb}$ . Using the cross-section results  
62 they have estimated the practical production possibility of  ${}^{161}\text{Tb}$ . Since their excitation  
63 function results showed discrepancies for the  ${}^{\text{nat}}\text{Gd}(d,xn){}^{160,161}\text{Tb}$  reactions, especially at  
64 lower energies (below 10 MeV), we found it necessary to re-measure these processes to  
65 get reliable cross-section databases for yield estimations. The limited number of their  
66 cross-section data for the  ${}^{\text{nat}}\text{Gd}(d,xn){}^{155,156}\text{Tb}$  reactions also motivated us to re-measure  
67 these reactions as well. The measured cross sections were also compared with the  
68 predictions by means of the TALYS code [14], according to the TALYS-based evaluated  
69 nuclear data library TENDL 2014.

## 70 **Experimental**

71 Natural Gd metal foils ( ${}^{152}\text{Gd}$ : 0.2 %,  ${}^{154}\text{Gd}$ : 2.18 %,  ${}^{155}\text{Gd}$ : 14.8 %,  ${}^{156}\text{Gd}$ : 20.47 %,  
72  ${}^{157}\text{Gd}$ : 15.65 %,  ${}^{158}\text{Gd}$ : 24.84 %,  ${}^{160}\text{Gd}$ : 21.86 %) with thicknesses of 8.61, 23.4  $\mu\text{m}$   
73 (obtained from Goodfellow Metals, UK) and 31.87  $\mu\text{m}$  (supplied by New Metals, UK),  
74 were used for the targets stacks. The thin metal Ti foils (10, 20 and 25  $\mu\text{m}$ ) which were  
75 employed for energy degradation and beam intensity monitoring were also supplied by  
76 Goodfellow. The cross-section data were collected in three separate experimental runs.  
77 The samples were irradiated in the form of stacks. In Debrecen two activations were

78 performed with energetic deuteron particles (10 MeV; both cases) accelerated by the  
79 MGC20 cyclotron of ATOMKI. The irradiations lasted 2.6 h and 2.06 h with beam  
80 currents of 50 nA in both cases. The investigated energy regions were 9.58 to 4.2 MeV.  
81 The stacks in Debrecen contained 5 and 5 Gadolinium foils of 31.87  $\mu\text{m}$ . In Japan one  
82 experiment was performed at the NIRS cyclotron with extracted deuteron energy of 30.24  
83 MeV. The beam current was 50 nA. The target consisted of five ‘thicker’ (thickness: 23.4  
84  $\mu\text{m}$ ) and four ‘thinner’ (thickness: 8.61  $\mu\text{m}$ ) Gadolinium foils. The 5 thick samples (and  
85 the degrader foils) slowed down the deuteron beam to 15.4 MeV while energy of the  
86 outgoing beam, leaving the last thin target, was 4.2 MeV. The beam current was  
87 measured via electric charge collection in a Faraday-cup at both laboratories. Good  
88 agreement between direct current measurements and results from deuteron monitor  
89 activations has consistently been obtained. For this purpose the reference cross-sections  
90 of the  $^{nat}\text{Ti}(d,xn)^{48}\text{V}$  monitor process have been used [15]. The induced radioactivity of  
91 the samples and monitor foils were measured non-destructively using HPGe detector  
92 gamma-ray spectrometry, analyzing the dominant gamma-rays of the investigated  
93 radionuclides. The accurately calibrated detectors had relative efficiencies of 10% and  
94 30%, (ATOMKI and NIRS respectively), with corresponding resolutions of 2.1 keV  
95 FWHM and 1.8 keV FWHM at 1.33 MeV. The photo-peak areas were determined using  
96 a quantitative analysis software package at NIRS (supplied by Laboratory Equipment  
97 Japan) and the FGM program at ATOMKI [16]. The decay data of  $^{155}\text{Tb}$ ,  $^{156}\text{Tb}$ ,  $^{160}\text{Tb}$  and  
98  $^{161}\text{Tb}$  and their dominant contributing reactions are collected in Table 1. The cross  
99 sections were calculated by applying the well-known activation formula. The total  
100 uncertainties of the measurements were calculated according to Gaussian error  
101 propagation and are given together with the cross-section data in Table 2. The errors of  
102 non-linear parameters (time etc.) were not considered but their contribution is negligible  
103 compared to the linear parameters. The average total cross-section uncertainty was  
104 around 14%. The uncertainty of the energy was estimated from the uncertainties of the  
105 primary incident deuteron beams and the target thicknesses taking also into account the  
106 energy straggling.

107

108 **Table 1.** Decay characteristic and contributing reactions for production of  $^{155}\text{Tb}$ ,  $^{156}\text{Tb}$ ,  
 109  $^{160}\text{Tb}$  and  $^{161}\text{Tb}$

Nuclide	Half-life (day)	Gamma energy used for identification (keV)	Contributing reaction	Q-value (MeV)
$^{155}\text{Tb}$	5.32	180.08 1340.67	$^{154}\text{Gd}(d,n)$ ,	2.61
			$^{155}\text{Gd}(d,2n)$	-3.83
			$^{156}\text{Gd}(d,3n)$	-12.36
$^{156}\text{Tb}$	5.35	534.29 1222.44	$^{157}\text{Gd}(d,4n)$	-18.72
			$^{155}\text{Gd}(d,n)$	3.09
			$^{156}\text{Gd}(d,2n)$	-5.45
			$^{157}\text{Gd}(d,3n)$	-11.81
$^{160}\text{Tb}$	72.3	879.38	$^{158}\text{Gd}(d,4n)$	-19.75
			$^{160}\text{Gd}(d,2n)$	-3.11
$^{161}\text{Tb}$	6.89	74.57	$^{160}\text{Gd}(d,n)$	4.58
			$^{160}\text{Gd}(d,p)$ $^{161}\text{Gd} \rightarrow ^{161}\text{Tb}$	-3.41

110 **Results and Discussion**

111 The measured cross sections for the formation of end products  $^{155}\text{Tb}$ ,  $^{156}\text{Tb}$ ,  $^{161}\text{Tb}$  and  
 112  $^{160}\text{Tb}$  are shown in Figs.1-4 and compared to the available literature results. Additionally,  
 113 theoretical curves taken from TENDL-2014 library (calculated by TALYS code) are also  
 114 added to the figures [14]. The presently measured cross-section values are also collected  
 115 in Table 2. Since we investigate here only the production possibilities at low energies, all  
 116 measured cross-section values above 22 MeV will be published separately.

117

118 *Excitation functions of the  $^{nat}\text{Gd}(d,xn)^{155,156}\text{Tb}$  nuclear processes*

119 Below 20 MeV three reactions ( $^{154}\text{Gd}(d,n)$ ,  $^{155}\text{Gd}(d,2n)$  and  $^{156}\text{Gd}(d,3n)$ ) contribute to the  
 120 formation  $^{155}\text{Tb}$  using natural Gd target. Due to this fact, it was possible to evaluate only  
 121 the ‘natural’ cross-sections for its formation. (Natural cross-section is the sum of cross  
 122 sections of the contributing nuclear reactions weighted by the natural isotopic abundance  
 123 of the target nucleus.)

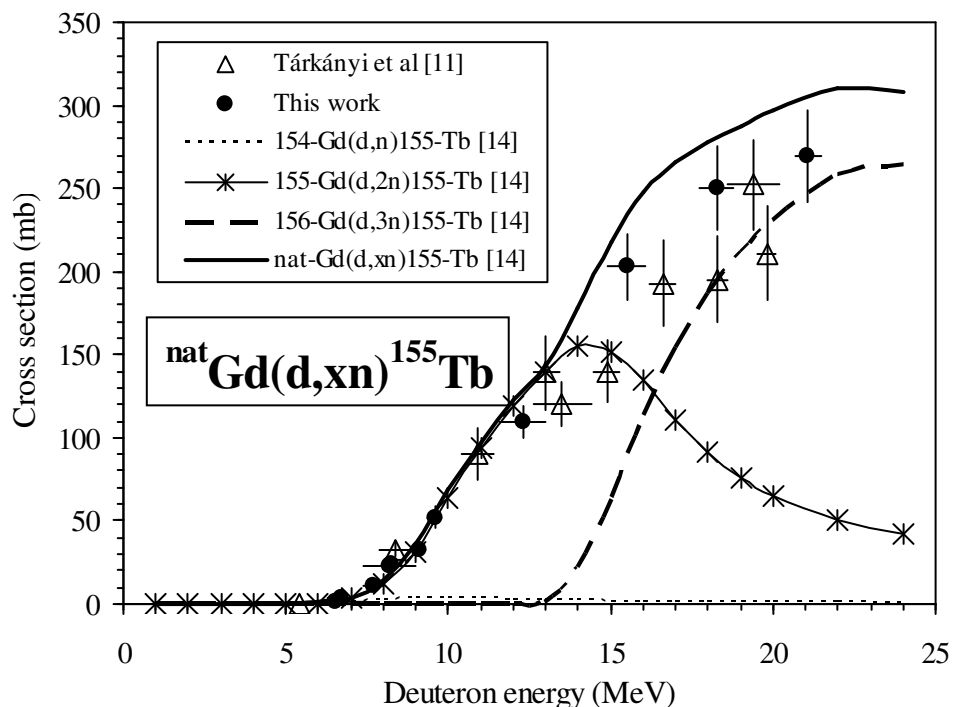
124 **Table 2.** Measured cross sections for the production of  $^{155,156,160,161}\text{Tb}$  radionuclides in  
 125 the irradiation of  $^{\text{nat}}\text{Gd}$  with deuterons

Deuteron energy (MeV)	Cross section (mb)			
	$^{155}\text{Tb}$	$^{156}\text{Tb}$	$^{160}\text{Tb}$	$^{161}\text{Tb}$
4.2±0.4	-	-	0.3±0.1	2.1±0.6
4.9±0.5	-	-	0.3±0.1	4.0±0.5
6.5±1.0	1.1±0.1	0.7±0.1	4.3±0.7	10.4±11.3
6.7±0.4	4.1±0.6	3.1±0.4	6.3±0.8	9.7±1.2
7.7±0.3	10.6±1.1	10.6±1.2	15.9±1.8	17.0±1.9
8.2±0.9	23.2±2.5	42.2±5.2	25.1±2.8	29.3±3.2
8.2±0.3	23.5±3.2	23.6±2.6	32.7±3.9	26.0±2.9
9.1±0.2	32.9±3.8	42.7±4.7	56.3±6.3	33.3±3.6
9.6±0.2	52.0±6.5	67.6±7.4	81.5±9.2	39.3±4.3
12.3±0.8	110±12	174±21	100±12	36.4±3.9
15.5±0.6	203±21	234±25	74.3±9.4	24.9±2.7
18.3±0.5	250±26	240±26	48.9±5.5	24.2±2.6
21.1±0.4	269±28	236±25	-	19.3±2.1

126

127 Our data are in good agreement with the values of Tárkányi *et al.* [11] over the whole  
 128 investigated energy region. The TENDL-2014 estimation for the  $^{\text{nat}}\text{Gd}+d$  process,  
 129 however, overpredict the experimental results especially above 13 MeV. The theoretical  
 130 excitation functions of the contributing reactions are also added to Fig.1. (The original  
 131 TENDL-2014 values were multiplied by us with the natural abundances of the target  
 132 nucleus in  $^{\text{nat}}\text{Gd}$ ). Taking into account the natural abundances of the possible targets, the  
 133 cross-section maximums and the available energy region, the  $^{155}\text{Gd}(d,2n)^{155}\text{Tb}$  reaction  
 134 would be useful for production purposes. Although the irradiation of  $^{\text{nat}}\text{Gd}$  could produce  
 135 useful amount of  $^{155}\text{Tb}$ , the co-formation of other (long-lived) Tb radioisotopes [11]  
 136 resulted in unacceptably high radioisotope contamination level of the final product. To  
 137 decrease this level, however, there is no other choice than using highly enriched  $^{155}\text{Gd}$   
 138 (>99.9) target. In this case the only major contamination would be  $^{156}\text{Tb}$  ( $T_{1/2} = 5.35$  d)  
 139 which is formed via the  $^{155}\text{Tb}(d,n)$  reaction. Unfortunately it has a half-live comparable to  
 140  $^{155}\text{Tb}$ , therefore it will be present in any final product. To estimate its formation  
 141 circumstances, we measured also the excitation function curve of the  $^{\text{nat}}\text{Gd}(d,xn)^{156}\text{Tb}$   
 142 process up to 21 MeV. The results can be seen in Fig.2. The cross sections of the

143 contributing processes, namely  $^{155}\text{Gd}(d,n)$ ,  $^{156}\text{Gd}(d,2n)$  and  $^{157}\text{Gd}(d,3n)$ , taken from the  
 144 TALYS-based evaluated nuclear data library TENDL 2014, are also added to Fig.2 [14].



145

146 **Fig.1.** Excitation functions for the production of  $^{155}\text{Tb}$  in the bombardment of  $^{\text{nat}}\text{Gd}$  with  
 147 deuterons

148 The present measurement is in relative good agreement with the data of Tárkányi *et al.*  
 149 [11]. However, the natural cross-section predictions of TENDL-2014 are closer to our  
 150 data especially in the energy range from 10 to 15 MeV.

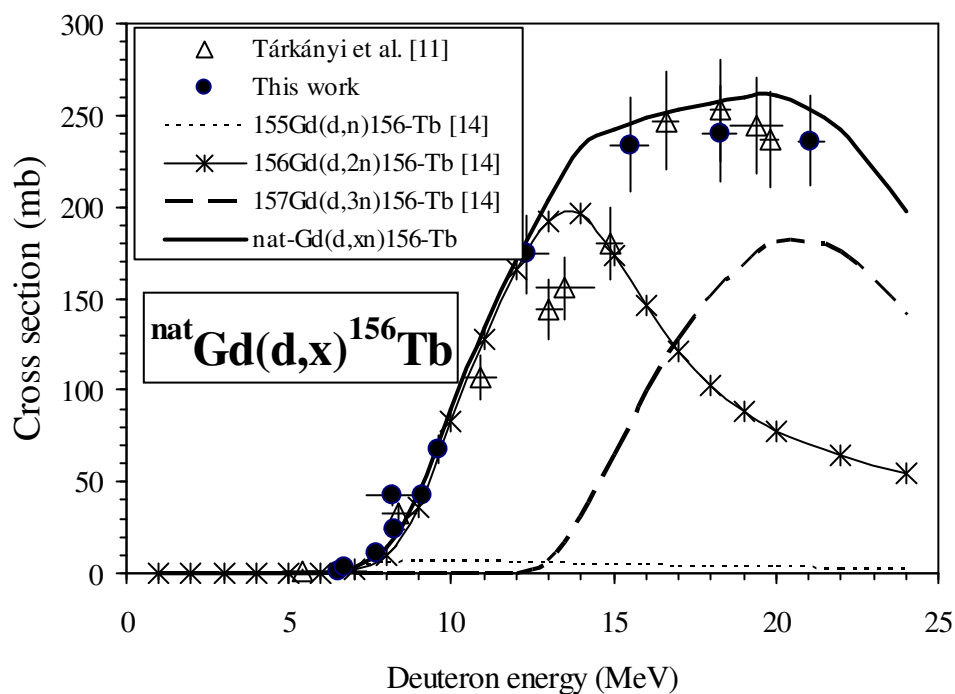
151 It can be seen that the impact of  $^{155}\text{Gd}(d,n)$  reaction to the production of  $^{156}\text{Tb}$  is almost  
 152 negligible. However, since the starting energies of the  $^{155}\text{Gd}(d,2n)$  and  $^{155}\text{Gd}(d,n)$  are  
 153 close to each other, there is no energy window where the  $^{155}\text{Tb}$  can be produced without  
 154  $^{156}\text{Tb}$  contamination even if 100% enriched target is used. The  $^{156}\text{Tb}/^{155}\text{Tb}$  contamination  
 155 level, using the theoretical (TALYS) excitation functions, strongly depends on the energy  
 156 window used for production. For example, at 14 MeV this contamination level is around  
 157 5 %.

158 Excitation functions of the  $^{nat}\text{Gd}(d,xn)^{161,160}\text{Tb}$  processes

159 The  $^{161}\text{Tb}$  is formed on one Gadolinium nuclide ( $^{160}\text{Gd}$ ) via a direct reaction

160 ( $^{160}\text{Gd}(d,n)^{161}\text{Tb}$ ) and through the decay of  $^{161}\text{Gd}$  ( $T_{1/2}= 3.66\text{ m}$ ) ( $^{160}\text{Gd}(d,p)^{161}\text{Gd}\rightarrow^{161}\text{Tb}$ )

161 in the case of deuteron activation.



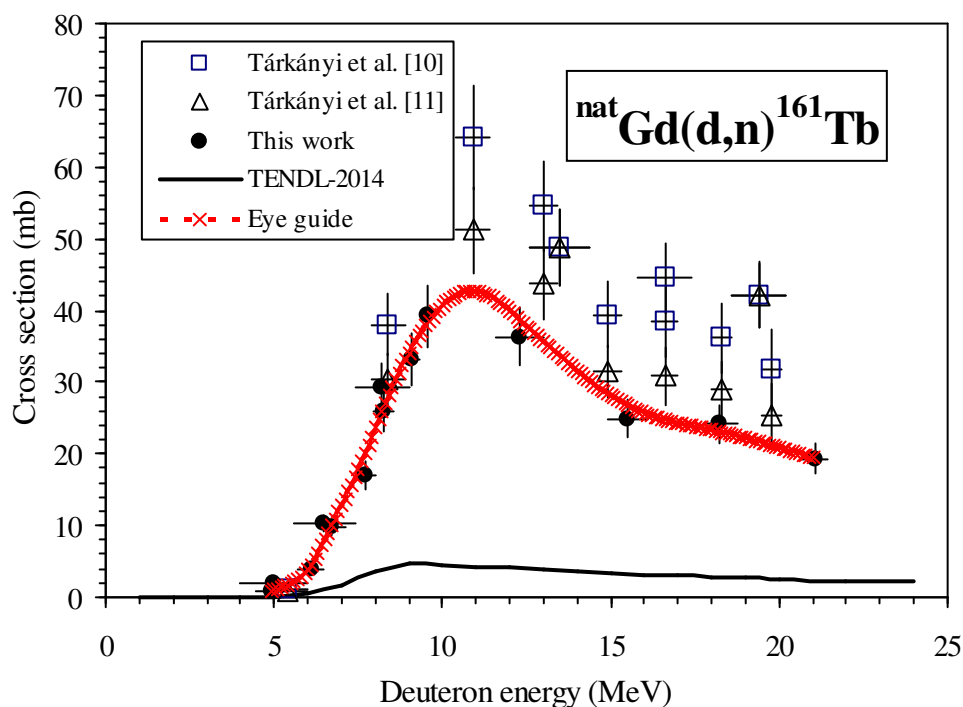
162

163 Fig.2. Excitation functions for the production of  $^{156}\text{Tb}$  in the bombardment of  $^{nat}\text{Gd}$  with  
164 deuterons

165 All cross-section values on Fig.3, including the present results are cumulative data  
166 calculated after the complete decay of the  $^{161}\text{Gd}$  precursor and refers to the natural  
167 isotopic abundance of  $^{160}\text{Gd}$  (21.86%). Our numerical cross-section data are collected in  
168 Table 2. The two data sets of Tárkányi *et al.* [10, 11] are also reproduced on this figure.  
169 Our excitation function seems to support the most recent result of Tárkányi *et al.* [11]. As  
170 usual in the case of  $(d,n)$  reactions in this mass region, the theoretical results published in  
171 TENDL-2014 library significantly underestimate the experimental values.



172 Based on the experimental results, this reaction seems to be useful for production  
 173 purposes if highly enriched (>99.9%)  $^{160}\text{Gd}$  is employed. Our calculation predicts  
 174 somewhat lower yields (10-15%) than it was reported by Tárkányi *et al.* in their first  
 175 article [10], but still acceptable for practical purposes.

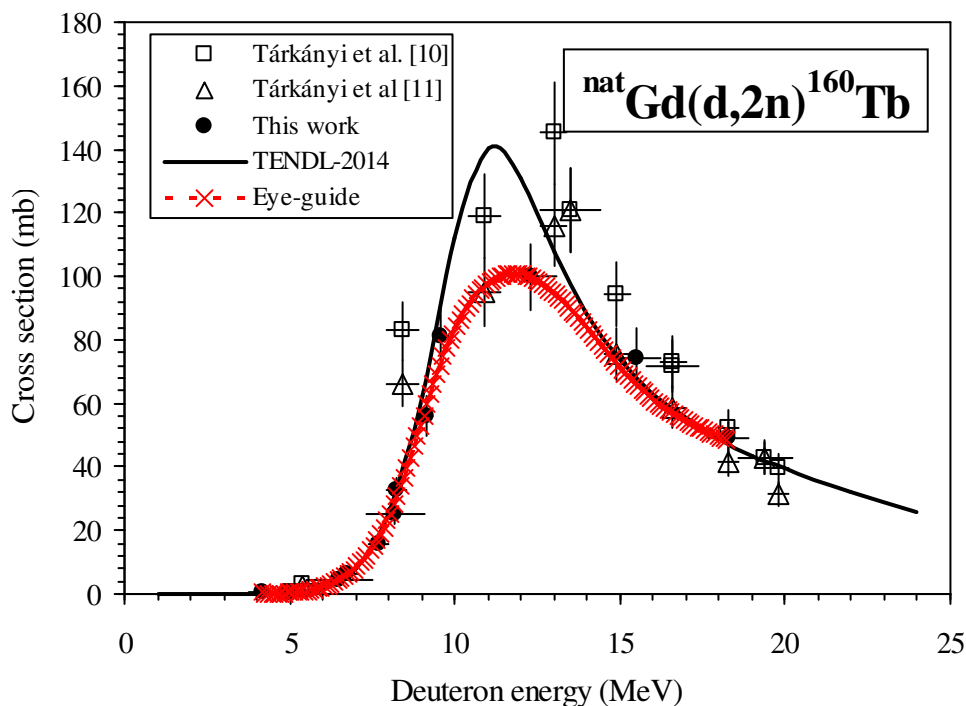


176

177 **Fig. 3.** Excitation functions for the production of  $^{161}\text{Tb}$  in the bombardment of  $^{nat}\text{Gd}$  with  
 178 deuterons

179 In the investigated energy range one radio-contaminant will be co-formed even if 100%  
 180 enriched  $^{160}\text{Gd}$  is used as target. Unfortunately this radioisotope ( $^{160}\text{Tb}$ ) has almost 10  
 181 times longer half-life than the  $^{161}\text{Tb}$  (see Table 1) therefore its influence can not be  
 182 neglected from the point of view of medical applications. We have also re-measured the  
 183 excitation function of the  $^{160}\text{Gd}(d,2n)^{160}\text{Tb}$  nuclear reaction, which only responsible for  
 184  $^{160}\text{Tb}$  formation. Our results together with the literature results and the predicted curve of  
 185 the TENDL-2014 calculation can be seen in Fig.4. (Note that all values refer to the  
 186 natural abundance of  $^{160}\text{Gd}$ ). While the present data support the most recent values of  
 187 Tárkányi *et al.* [11], the theoretical calculation seems to show better agreement with the  
 188 earlier literature values [10]. The recent cross-section results for both of the above

189 investigated reactions confirm the conclusion reported in [10]: Due to the high level of  
 190 the  $^{160}\text{Tb}$  contamination in the final product there is no energy window where the  $^{161}\text{Tb}$   
 191 can be produced for medical purposes.



192

193 **Fig. 4.** Excitation functions for the production of  $^{160}\text{Tb}$  in the bombardment of  $^{\text{nat}}\text{Gd}$  with  
 194 deuterons

195 Since the number of the co-produced  $^{160}\text{Tb}$  is much higher (around twice) than the  $^{161}\text{Tb}$ ,  
 196 this production route seems to be useful only for developmental studies. Note that the  
 197  $^{160}\text{Tb}/^{161}\text{Tb}$  contamination level increases as function of irradiation time.

198 **Conclusion**

199 The detailed cross-section measurement of this work not only extended the databases of  
 200 the  $^{\text{nat}}\text{Gd}(d, xn)^{155,156,160,161}\text{Tb}$  nuclear processes up to 21 MeV, but also pointed to the  
 201 disagreement between the experimentally measured data of the literature. Cross-section  
 202 results revealed that both  $^{155}\text{Tb}$  and  $^{161}\text{Tb}$  can not be produced in no-carrier-added form

203 even using 100% enriched  $^{155}\text{Gd}$  and  $^{160}\text{Gd}$  targets, respectively. Their practical  
204 application therefore is limited to supply radioactive Terbium for developmental studies.  
205 At present the only practical method for production of medically relevant  $^{161}\text{Tb}$   
206 radioisotope is the spallation-type reaction followed by mass separation.

## 207 **Acknowledgements**

208 The Hungarian authors wish to thank the financial support by the Hungarian Research  
209 Foundation, (Budapest, OTKA K108669).

## 210 **References**

- 211 1. Müller C, Zhernosekov K, Köster U, Johnston K, Hohn A, van der Walt TN, Türler  
212 A, Schibli R (2012) A unique matched quadruplet of terbium radioisotopes for PET  
213 and SPECT and for  $\alpha$ - and  $\beta^-$ -radionuclide therapy: An in vivo proof-of-concept  
214 study with a new receptor-targeted folate derivative, *J. Nucl. Med.* 53: 1951
- 215 2. Dmitriev PP, Molin GA, Dmitrieva ZP (1989) The production of  $^{155}\text{Tb}$  for nuclear  
216 medicine by  $^{155}\text{Gd}(p,n)$ ,  $^{156}\text{Gd}(p,2n)$ ,  $^{155}\text{Gd}(d,2n)$  *Atomnaya Energija*, 66: 419
- 217 3. Rizvi L, Abbas SM, Sarkar S, Goozee G (2000) Radio-immunoconjugates for targ-  
218 eted [alpha] therapy of malignant melanoma, *Melanom. Research* 10: 281
- 219 4. Becker CFW, Clayton D, Shapovalov G, Lester HA, Kochendoerfer GG (2004) On-  
220 resin assembly of a linkerless lanthanide(III)-based luminescence label and its  
221 application to the total synthesis of site-specifically labeled mechanosensitive  
222 channels. *Bioconj Chem* 15: 1118
- 223 5. Levin VI, Malanin AB, Tronova IN (1981) Production of radionuclides by  
224 photonuclear reactions. I. Production of terbium-155 and thulium-167 using the  
225 electron accelerator EA-25, *Radiochem. Radioanal. Lett.* 49: 111
- 226 6. Qaim SM (2001) Therapeutic radionuclides and nuclear data *Radiochim Acta* 89:297
- 227 7. Zaitseva NG, Dmitriev SN, Maslov OD, Molokanov LG, Starodub YA, Shishkin  
228 SV, Shishkina TV (2003) Terbium-149 for nuclear medicine. The production of  $^{149}\text{Tb}$   
229 via heavy ions induced nuclear reactions, *Czech J Phys*, Vol. 53: A455

- 230 8. Maiti M (2011) New measurement of cross sections of evaporation residues from the  
231  $^{nat}\text{Pr} + ^{12}\text{C}$  reaction: A comparative study on the production of  $^{149}\text{Tb}$ , Phys Rev C 84:  
232 044615
- 233 9. Maiti, M, Susanta L, Tomar BS (2011) Investigation on the production and isolation  
234 of  $^{149,150,151}\text{Tb}$  from  $^{12}\text{C}$  irradiated natural praseodymium target, Radiochim Acta  
235 99:527
- 236 10. Tárkányi F, Hermanne A, Takács S, Ditrói F, Csikai J, Ignatyuk AV (2013) Cross-  
237 section measurement of some deuteron induced reactions on  $^{160}\text{Gd}$  for possible  
238 production of the therapeutic radionuclide  $^{161}\text{Tb}$ . Radioanal Nucl Chem 298:1385
- 239 11. Tárkányi F, Takács S, Ditrói F, Hermann A, Ignatyuk AV (2014) Activation cross-  
240 sections of longer-lived radioisotopes of deuteron induced nuclear reactions on  
241 terbium up to 50 MeV Nucl Instrum Meth B316:183
- 242 12. Steyn GF, Vermeulen C, Szelecsényi F, Kovács Z, Hohn A, van der Meulen NP,  
243 Schibli R, van der Walt TN (2014) Cross sections of proton-induced reactions on  
244  $^{152}\text{Gd}$ ,  $^{155}\text{Gd}$  and  $^{159}\text{Tb}$  with emphasis on the production of selected Tb radionuclides  
245 Nucl Instrum Meth B 319:128
- 246 13. Vermeulen C, Steyn GF, Szelecsényi F, Kovács Z, Suzuki K, Nagatsu K, Fukumura  
247 T, Hohn A, van der Walt TN (2012) Cross sections of proton-induced reactions on  
248  $^{nat}\text{Gd}$  with special emphasis on the production possibilities of  $^{152}\text{Tb}$  and  $^{155}\text{Tb}$  Nucl  
249 Instrum Meth B 275: 24
- 250 14. Koning AJ, Rochman D, van der Marck D, Kopecký SJ, Sublet JCh, Pomp S,  
251 Sjöstrand H, Forrest R, Bauge E, Henriksson H, Cabellos O, Goriely S, Leppanen J,  
252 Leeb H, Plompen A, Mills R (2014) TENDL 2014: TALYS-based evaluated nuclear  
253 data library, available from [www.talys.eu](http://www.talys.eu)
- 254 15. Gul K, Hermanne A, Mustafa MG, Nortier FM, Obložinsky P, Qaim SM, Scholten  
255 B, Shubin Y, Takács S, Tárkányi FT, Zhuang Z Charged particle cross-section  
256 database for medical radioisotope production: diagnostic radioisotopes and monitor  
257 reactions. IAEA-TECDOC-1211, IAEA, Vienna, Austria. Available from URL:  
258 <<http://www-nds.iaea.org/medical/>>
- 259 16. Székely G (1985) FGM – a flexible gamma-spectrum analysis program for a small  
260 computer Comput. Phys. Commun. 34: 313